JCB Article

Regulation of Rac1 activation by the low density lipoprotein receptor–related protein

Zhong Ma,[1] Keena S. Thomas,[1] Donna J. Webb,[3] Radim Moravec,[2] Ana Maria Salicioni,[1] Wendy M. Mars,[4] and Steven L. Gonias[1,2]

[1]Department of Pathology, [2]Department of Biochemistry and Molecular Genetics, and [3]Department of Cell Biology, University of Virginia School of Medicine, Charlottesville, VA 22908
[4]Department of Pathology, University of Pittsburgh School of Medicine, Pittsburgh, PA 15261

The low density lipoprotein receptor–related protein (LRP-1) binds and mediates the endocytosis of multiple ligands, transports the urokinase-type plasminogen activator receptor (uPAR) and other membrane proteins into endosomes, and binds intracellular adaptor proteins involved in cell signaling. In this paper, we show that in murine embryonic fibroblasts (MEFs) and L929 cells, LRP-1 functions as a major regulator of Rac1 activation, and that this activity depends on uPAR. LRP-1–deficient MEFs demonstrated increased Rac1 activation compared with LRP-1–expressing MEFs, and this property was reversed by expressing the VLDL receptor, a member of the same gene family as LRP-1, with overlapping ligand-binding specificity. Neutralizing the activity of LRP-1 with receptor-associated protein (RAP) increased Rac1 activation and cell migration in MEFs and L929 cells. The same parameters were unaffected by RAP in uPAR−/− MEFs, prepared from uPAR gene knockout embryos, and in uPAR-deficient LM-TK$^-$ cells. Untreated uPAR+/+ MEFs demonstrated substantially increased Rac1 activation compared with uPAR−/− MEFs. In addition to Rac1, LRP-1 suppressed activation of extracellular signal–regulated kinase (ERK) in MEFs; however, it was Rac1 (and not ERK) that was responsible for the effects of LRP-1 on MEF migration. Thus, LRP-1 regulates two signaling proteins in the same cell (Rac1 and ERK), both of which may impact on cell migration. In uPAR-negative cells, LRP-1 neutralization does not affect Rac1 activation, and other mechanisms by which LRP-1 may regulate cell migration are not unmasked.

Introduction

Receptors in the low density lipoprotein receptor gene family (LRFs)* are type I transmembrane proteins with common structural modules, including EGF-like repeats, complement-like repeats, and YWTD-containing repeats (Strickland et al., 2002). LRFs may localize to clathrin-coated pits and/or caveolae and typically undergo constitutive endocytosis and recycling (Goldstein et al., 1979; Weaver et al., 1996; Li et al., 2001; Boucher et al., 2002). Some of the better-characterized LRFs, including the low density lipoprotein receptor–related protein (LRP-1), gp330/megalin (LRP-2), and the VLDL receptor (VLDLr) bind multiple ligands with partially overlapping specificity, including proteinases, proteinase–inhibitor complexes, ECM proteins, hormones, growth factors, and foreign proteins (Strickland et al., 2002). Bound ligands are internalized and then usually transported to lysosomes for degradation.

LRFs frequently bind proteins that are already associated with other cell-surface receptors or binding sites in the same cell. For example, protease nexin 1–proteinase complexes bind first to heparan sulfate proteoglycans and then to LRP-1 (Knauer et al., 1997). Urokinase-type plasminogen activator (uPA)–plasminogen activator inhibitor-1 (PAI-1) complex, which forms in association with the uPA receptor (uPAR), rapidly binds to LRP-1 or the VLDLr (Conese et al., 1995; Webb et al., 1999). Similarly, factor VIIa–tissue factor pathway inhibitor complex, which forms in association with tissue factor, binds to LRP-1 (Hamik et al., 1999). In these examples, LRP-1 internalizes not only the ligand, but may also internalize the bridged receptor and thereby decrease the level of the second receptor in the plasma membrane. The plasma

Address correspondence to Steven L. Gonias, Dept. of Pathology, University of Virginia School of Medicine, Box 800214, Charlottesville, VA 22908. Tel.: (434) 924-9192. Fax: (434) 982-0283.
E-mail: slg2t@virginia.edu

*Abbreviations used in this paper: ERK, extracellular signal–regulated kinase; GPI, glycosylphosphatidylinositol; LRF, receptor in the low density lipoprotein receptor gene family; LRP-1, low density lipoprotein receptor–related protein; MEF, murine embryonic fibroblast; MLCK, myosin light chain kinase; PAI-1, plasminogen activator inhibitor-1; RAP, receptor-associated protein; uPA, urokinase-type plasminogen activator; uPAR, uPA receptor; VLDLr, VLDL receptor; VLK-*p*NA, *H*-D-Val-L-Leu-L-Lys-*p*-nitroanilide.

Key words: urokinase-type plasminogen activator; uPAR; extracellular signal–regulated kinase; cell migration; VLDL receptor

membrane–associated proteinase inhibitor, amyloid precursor protein (APP), undergoes LRP-1–facilitated endocytosis due to two distinct interactions, the first involving the extracellular domains of APP and LRP-1, which associate after APP binds proteinase; and the second involving intracytoplasmic domains of APP and LRP-1, which are bridged by the bifunctional adaptor protein, Fe65 (Ulery et al., 2000; Kinoshita et al., 2001). By these mechanisms, LRP-1 remodels the plasma membrane and may indirectly regulate the ability of the cell to respond to growth factors and other regulatory molecules.

LRFs also function as signaling coreceptors for diverse ligands. The VLDLr and apoER2 are essential components of the reelin-initiated cell signaling pathway that controls development of the central nervous system (D'Arcangelo et al., 1999; Trommsdorff et al., 1999). Similarly, LRP-6 functions as a coreceptor in Wnt signaling (Tamai et al., 2000). NPxY motifs, which are found in the intracytoplasmic domains of many LRFs, bind proteins involved in cell signaling, including Dab-1, Fe65, Shc, Jun kinase–interacting protein, and ced-6/GULP (Gotthardt et al., 2000; Barnes et al., 2001; Su et al., 2002). These interactions, which are regulated by NPxY tyrosine phosphorylation, may promote activation of signaling proteins or sequester signaling proteins, preventing their transfer to effector sites such as the nucleus.

In murine embryonic fibroblasts (MEFs) and HT 1080 fibrosarcoma cells, loss of LRP-1 expression is associated with increased uPA accumulation in the medium, increased cell surface uPAR, and increased cell migration on vitronectin-coated surfaces (Weaver et al., 1997; Webb et al., 2000). Similar changes are observed when the activity of the VLDLr is neutralized in MCF-7 breast cancer cells (Webb et al., 1999). In the HT 1080 and MCF-7 cells, uPA and uPAR establish an autocrine signaling pathway in which Ras and extracellular signal–regulated kinase (ERK) are activated (Ossowski and Aguirre-Ghiso, 2000; Webb et al., 2000). ERK and its downstream effector, myosin light chain kinase (MLCK), are responsible for the increase in cell migration (Nguyen et al., 1999; Webb et al., 2000); however, ERK does not control cell migration in all cell types. Factors that may influence whether cell migration is regulated by ERK include integrin expression and the biochemical composition of the migration substratum (Yebra et al., 1996; Klemke et al., 1997; Nguyen et al., 1999).

The function of LRP-1 as a regulator of cell-surface uPAR suggests mechanisms other than activation of the Ras–ERK pathway whereby LRP-1 may affect cell migration. Kjoller and Hall (2001) demonstrated that uPAR overexpression promotes cell migration by activating the small GTPase, Rac1. This effect did not require uPA, but instead involved direct binding of uPAR to vitronectin, a previously documented uPAR ligand (Wei et al., 1994). Activated Rac1 regulates the activity of terminal effector proteins such as Arp2/3 complex, cofilin, and actin capping protein to initiate and stabilize new actin polymerization in advancing lamellipodia of the migrating cell (Kraynov et al., 2000; Ridley, 2001). Other mechanisms by which LRP-1 may regulate cell migration that are independent of uPAR include the recently demonstrated interaction of LRP-1 with platelet-derived growth factor BB (Loukinova et al., 2002) and the function of LRP-1 in regulating fibronectin accumulation in association with cells (Salicioni et al., 2002).

In this work, our major goals were to determine whether LRP-1 regulates cell signaling through pathways other than the Ras–ERK pathway and to identify novel mechanisms whereby LRP-1 may control cell migration. To accomplish these goals, it was essential to distinguish between pathways that depend on uPAR and those that do not. Thus, we prepared uPAR−/− MEFs from embryos of crossbred heterozygous uPAR gene knockout mice. These cells demonstrated substantially decreased Rac1 activation compared with uPAR+/+ MEFs, suggesting that uPAR regulates Rac1 when expressed at normal levels, as well as when it is overexpressed (Kjoller and Hall, 2001). Because LRP-1 down-regulates cell-surface uPAR, LRP-1–deficient MEFs and cells that were cultured in the presence of receptor-associated protein (RAP) to neutralize the activity of LRP-1 (Webb et al., 1999) demonstrated substantially increased Rac1 activation. Expression of the VLDLr in LRP-1–deficient MEFs decreased Rac1 activation. When LRP-1 activity was neutralized in uPAR-deficient cells, including uPAR−/− MEFs and LM-TK$^-$ fibroblasts, Rac1 activation and cell migration were unaffected. Thus, LRP-1 does not regulate MEF/fibroblast migration by uPAR-independent mechanisms that are masked when uPAR is expressed.

Results

Rac1 is suppressed in uPAR−/− MEFs

Kjoller and Hall (2001) demonstrated that Rac1 is activated in cells that overexpress uPAR. Because LRP-1 regulates the level of cell-surface uPAR by promoting uPAR endocytosis and catabolism (Conese et al., 1995; Webb et al., 2000), we hypothesized that LRP-1 may function as a major regulator of the basal level of Rac1 activation. To study the relationship between uPAR and LRP-1 in Rac1 activation, heterozygous (uPAR+/−) mice were bred and MEFs were isolated from the embryos. A1 (uPAR−/−), B1 (uPAR+/−), and C1 (uPAR+/+) cells were derived from littermates. A second cell line with each genotype (uPAR−/− A2 cells, uPAR+/− B2 cells, and uPAR+/+ C2 cells) was isolated from separate matings.

Fig. 1 A shows a representative semi-quantitative PCR analysis of the uPAR allele in A1, B1, and C1 cells. Because murine uPAR-specific antibodies are not highly effective, we used a previously described functional assay to quantitate cell-surface uPAR (Weaver et al., 1997). The uPAR was loaded with murine uPA, which was then detected based on its ability to activate plasminogen. Under the conditions of our assay, plasminogen activation and *H*-D-Val-L-Leu-L-Lys-*p*-nitroanilide (VLK-*p*NA) hydrolysis are linear functions of the concentration of cell-associated uPA. We confirmed that plasminogen activation was due to uPA, using the uPA-specific inhibitor amiloride (Weaver et al., 1997). Fig. 1 B shows that cell-associated uPA was nearly undetectable in the uPAR−/− cells. Interestingly, the uPAR+/− cells bound <50% of the uPA retained by uPAR+/+ cells. As shown in Fig. 1 C, uPAR expression did not affect LRP-1 expression.

Transwell migration assays were performed using membranes coated on the bottom surface with vitronectin. 10%

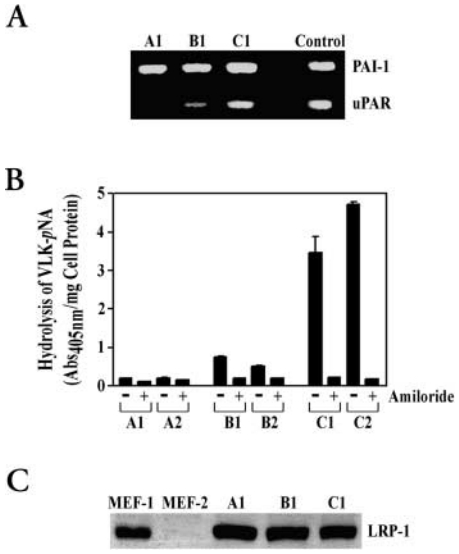

Figure 1. **Characterization of uPAR-deficient MEFs.** (A) Genomic DNA PCR was performed to detect the intact uPAR allele in A1, B1, and C1 cells, using primers that hybridize with exon 3 of the uPAR gene. The PAI-1 allele was also detected as an internal control for total DNA. The lane labeled "control" shows DNA from the tail of a normal mouse. (B) Cell-surface uPAR in uPAR−/− (A1 and A2), uPAR+/− (B1 and B2), and uPAR+/+ (C1 and C2) cells was detected by plasminogen activation assay. 0.5 mM amiloride was added to some cultures to inhibit uPA-specific plasminogen activation. Substrate hydrolysis was standardized based on cell protein. (C) Expression of LRP-1 in uPAR−/− (A1), uPAR+/− (B1), and uPAR+/+ (C1) cells and in MEF-1 (LRP-1-positive) and MEF-2 (LRP-1-negative) cells was detected by immunoblot analysis using an antibody 11H4.

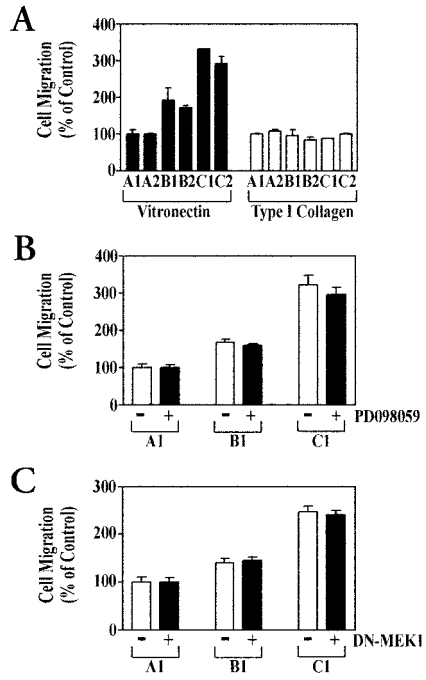

Figure 2. **Migration of uPAR-deficient MEFs.** (A) uPAR−/− (A1 and A2), uPAR+/− (B1 and B2), and uPAR+/+ (C1 and C2) MEFs were allowed to migrate through Transwell membranes that were precoated with purified vitronectin or type I collagen. Migrating cells were detected by crystal violet staining. (B) uPAR−/− (A1), uPAR+/− (B1), and uPAR+/+ (C1) MEFs were treated with DMSO (−) or 10 μM PD098059 (+) for 15 min at RT and then allowed to migrate through Transwell membranes that were precoated with 20% FBS. Migrating cells were detected by crystal violet staining. (C) A1, B1, and C1 MEFs were cotransfected to express dominant-negative MEK1 (DN-MEK1) and pEGFP-N1. Control cells were cotransfected with equal amounts of empty vector (pBK-CMV) and pEGFP-N1. After culturing for 24 h, the cells were allowed to migrate for 4 h through serum-coated membranes. Migration was determined by fluorescence microscopy. Results are expressed relative to the migration rate of A1 cells that were cotransfected with pBK-CMV and pEGFP-N1 (mean ± SEM).

FBS was added to the lower migration chamber. Under these conditions, MEF migration correlated with uPAR expression (Fig. 2 A). uPAR+/+ cells migrated more rapidly than uPAR+/− cells, which in turn migrated more rapidly than uPAR−/− cells. By contrast, uPAR expression did not affect MEF migration on type I collagen. A selective relationship in which the uPA–uPAR system promotes cell migration on vitronectin and not type I collagen has been observed previously in MCF-7 cells and in LRP-1–deficient MEF-2 cells (Weaver et al., 1997; Nguyen et al., 1999).

Binding of uPA to uPAR activates ERK, and this pathway is responsible for the effects of uPA on migration of MCF-7 and HT 1080 cells (Nguyen et al., 1999; Webb et al., 2000). To test whether ERK activation is responsible for the differences in migration of uPAR-positive and -negative MEFs, we pretreated A1, B1, and C1 cells with the MEK antagonist, PD098059. As shown in Fig. 2 B, PD098059 did not affect MEF migration, irrespective of the number of copies of the uPAR allele. Equivalent results were obtained with A2, B2, and C2 cells (not depicted). Dominant-negative MEK1 also failed to affect MEF migration, irrespective of the uPAR expression level (Fig. 2 C).

Next, we tested whether uPAR expression affects Rac1 activation in MEFs. We used an affinity pulldown assay to detect GTP-loaded Rac1. Fig. 3 A shows that two separate uPAR+/+ cell lines (C1 and C2) demonstrated significantly increased levels of GTP-Rac1, compared with uPAR−/− cells (A1 and A2). Furthermore, dominant-negative Rac1 (N17Rac1) selectively inhibited migration of the uPAR+/+ cells (Fig. 3 B). When Rac1-dependent signaling was antagonized, migration of uPAR+/+ and uPAR−/− cells was equivalent. These results demonstrate that naturally occurring uPAR regulates Rac1 activation, and that this activity is responsible for the effects of uPAR on MEF migration. The reason why inhibitors of ERK activation do not affect MEF migration has not been definitively determined; however, the level of endogenously produced uPA may be insufficient. Furthermore, we have shown that MEFs express $\alpha_V\beta_3$ and use this integrin for adhesion to vitronectin (unpublished data). Previous studies have shown that activated ERK is selective in promoting cell migration that is mediated by $\alpha_v\beta_5$ and not $\alpha_v\beta_3$ (Yebra et al., 1996; Klemke et al., 1997; Nguyen et al., 1999).

As further confirmation regarding the effects of uPAR on Rac1 activation, we examined the morphology of uPAR+/+ and uPAR−/− cells at various times after plating in FBS-precoated chamber slides. As shown in Fig. 4, both cell types adopted spread morphologies within 1 h; however, very few protrusions were seen in uPAR−/− cells. By contrast,

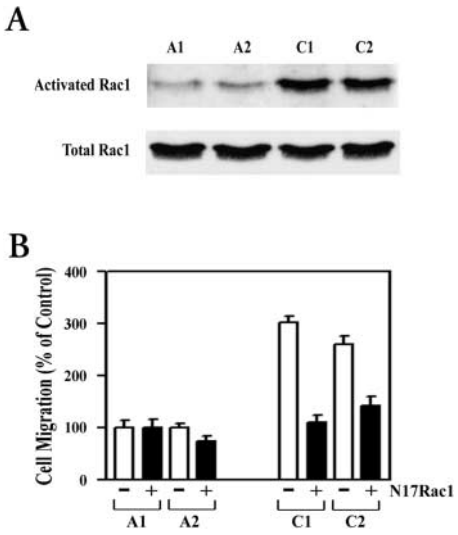

Figure 3. **uPAR regulates Rac1 activation in MEFs.** (A) uPAR−/− (A1 and A2) and uPAR+/+ (C1 and C2) MEFs were cultured in serum-supplemented medium for 18 h and then extracted to detect GTP-loaded Rac1. (B) uPAR−/− (A1 and A2) and uPAR+/+ (C1 and C2) MEFs were cotransfected with constructs encoding N17Rac1 and pEGFP-N1 or with pBK-CMV (empty vector) and pEGFP-N1. Cell migration was studied using serum-coated membranes. Migration was determined by fluorescence microscopy. Results are expressed relative to the migration rate of A1 cells that were cotransfected with pBK-CMV and pEGFP-N1 (mean ± SEM).

uPAR+/+ cells exhibited a polarized morphology with clearly defined leading lamellipodia. The motile phenotype, which was adopted only by uPAR+/+ cells, is consistent with the demonstrated activation of Rac1 in uPAR-expressing cells.

LRP-1 suppresses basal levels of activated ERK and Rac1

Although we previously demonstrated that LRP-1–deficient embryonic fibroblasts (MEF-2 cells) migrate more rapidly than LRP-1–expressing MEFs (Weaver et al., 1997), this difference was not explained by a change in cell signaling. Fig. 5 shows the results of experiments comparing the levels of ERK activation in MEF-1 and MEF-2 cells. Phosphorylated ERK was equivalent in MEF-1 and MEF-2 cells when FBS was present; however, when the cells were serum-deprived for 18 h, the level of phosphorylated ERK was significantly higher in the MEF-2 cells. Fig. 5 B shows ERK phosphorylation in MEF-2 cells as a function of time after serum withdrawal. Initially, ERK phosphorylation drops precipitously, but then recovers to near the level observed in the presence of serum. This pattern is consistent with a model in which an autocrine signaling pathway is established, involving ligands that accumulate in the absence of LRP-1. Although we did not attempt to identify a responsible ligand or ligands, the uPA–uPAR system has been characterized as a potent autocrine signaling system leading to ERK activation (Aguirre-Ghiso et al., 1999; Ma et al., 2001). Because uPA accumulates to greatly increased levels in the medium of MEF-2 cells compared with MEF-1 cells (Weaver et al., 1997), it is likely that the uPA–uPAR system is at least partially responsible for the increase in ERK phosphorylation in LRP-1–deficient MEF-2 cells after serum withdrawal.

Next, we compared the levels of activated Rac1 in MEF-1 and MEF-2 cells that were plated in serum-containing medium and cultured for 18 h. As shown in Fig. 6 A, the level of activated Rac1 was increased in the MEF-2 cells, relative to the MEF-1 cells, by 3.1 ± 0.8-fold. The increase in activated Rac1 was statistically significant ($P < 0.05$, $n = 6$).

The VLDLr and LRP-1 function equivalently as regulators of the uPA–uPAR system (Webb et al., 2000) and demonstrate substantial overlap in ligand-binding specificity (Strickland et al., 2002). To confirm the role of LRP-1 as a regulator of Rac1 activation in MEFs, we transfected MEF-2 cells to express the VLDLr. Immunoblot analysis was used to confirm VLDLr expression (Fig. 6 B). GTP-loaded Rac1 was decreased by 64 ± 7% in the VLDLr-expressing cells. This value represents a minimum estimate because we analyzed complete cultures in which probably only ~80% of the cells expressed the VLDLr. Thus, the VLDLr reversed the phenotype associated with LRP-1 deficiency, suppressing Rac1 activation in the MEF-2 cells.

To determine whether uPAR is required in the mechanism by which LRP-1 regulates Rac1, we cultured uPAR+/+ and uPAR−/− MEFs in the presence of RAP for 3 d. RAP

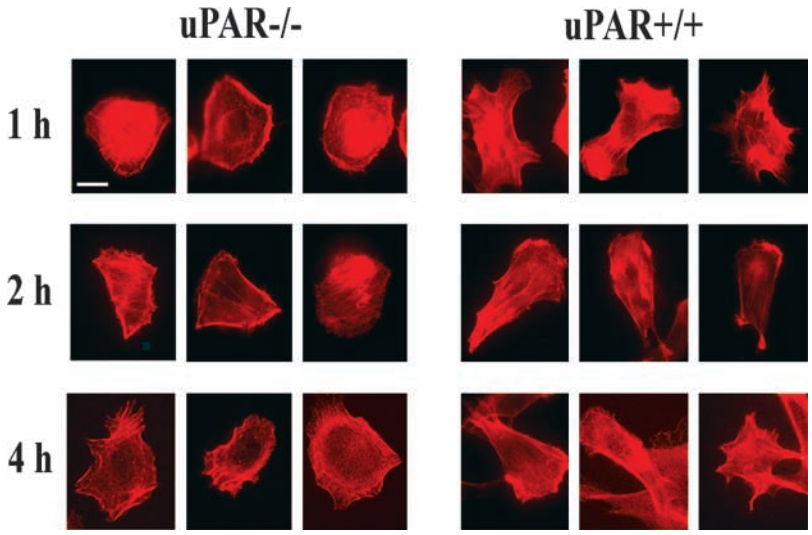

Figure 4. **uPAR expression alters the morphology of MEFs.** uPAR+/+ C1 cells and uPAR−/− A1 cells were plated in serum-coated chamber slides for the indicated times and stained with rhodamine-conjugated phalloidin. Images were collected by fluorescence microscopy. Bar, 10 μm.

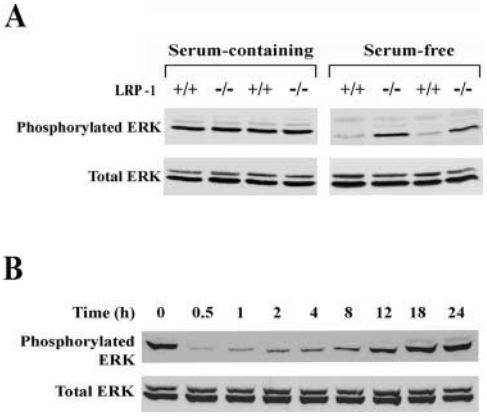

Figure 5. **LRP-1 expression suppresses ERK activation in serum-deprived MEFs.** (A) MEF-1 (LRP+/+) and MEF-2 (LRP−/−) cells were extracted without serum deprivation or after serum deprivation for 18 h. Phosphorylated and total ERK were detected by immunoblot analysis. (B) ERK phosphorylation in MEF-2 cells was determined as a function of time after serum deprivation.

neutralizes the ligand-binding activity of LRP-1, and as a result, up-regulates specific proteins in the plasma membrane, including uPAR (Webb et al., 1999). As shown in Fig. 6 C, RAP significantly increased the level of GTP-loaded Rac1 only in the uPAR+/+ MEFs ($P < 0.05$). No increase in Rac1 activation was observed in the uPAR−/− cells, suggesting that uPAR is essential for the regulation of Rac1 by LRP-1.

As a second model system to examine the effects of sustained LRF neutralization on Rac1 activation and to further test the role of uPAR, we cultured L929 and LM-TK$^-$ cells in the presence or absence of RAP for 3 d. LM-TK$^-$ cells are derived from L929 cells, but have lost genes encoding essential products for anchoring glycosylphosphatidylinositol (GPI)-linked proteins (Singh et al., 1991). We confirmed that L929 cells express cell-surface uPAR and that LM-TK$^-$ cells do not using our plasminogen activation assay (not depicted). Fig. 6 D shows that RAP increased Rac1 activation in the L929 cells ($P < 0.05$) but not in the LM-TK$^-$ cells. Again, these results are consistent with a model in which LRP-1 regulates Rac1 by a mechanism that requires uPAR.

LRP-1 regulates MEF migration by suppressing Rac1 activation

Images of phalloidin-stained MEF-1 and MEF-2 cells are shown in Fig. 7. LRP-1–deficient MEF-2 cells spread rapidly and then developed numerous lamellipodia that were obvious within 4 h of plating. By contrast, MEF-1 cells required more time to spread. By 4 h, most of the MEF-1 cells had adopted a spread phenotype; however, these cells demonstrated fewer well-developed lamellipodia. The difference in MEF phenotype is consistent with the selective activation of Rac1 in MEF-2 cells.

In Transwell migration assays, MEF-2 cells migrated more rapidly than MEF-1 cells (Fig. 8), confirming the results of our previously reported monolayer denudation experiments (Weaver et al., 1997). PD098059 and dominant-negative MEK1 failed to significantly affect migration of

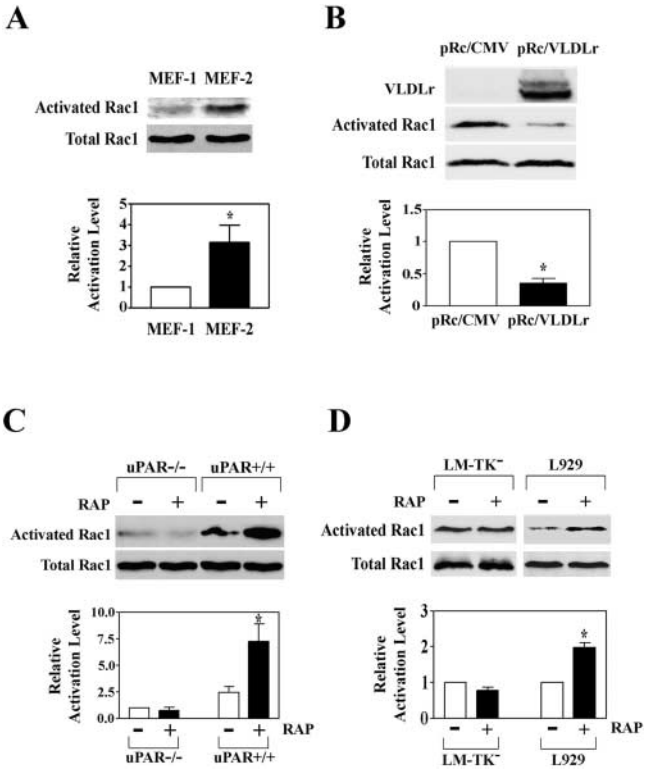

Figure 6. **LRP-1 suppresses Rac1 activation.** (A) MEF-1 and MEF-2 cells were cultured in DME and 10% FBS for 18 h and then extracted to detect activated and total Rac1. The level of activated Rac1 (standardized based on total Rac1) was determined by densitometry scanning using ImageQuant software to generate the values shown in the bar graph (mean ± SEM, $n = 3$). The asterisk indicates statistical significance (unpaired t test, $P < 0.05$). (B) MEF-2 cells were transfected to express VLDLr or with empty vector (pRc/CMV). Expression of the VLDLr and Rac1 activation were determined 4 d later. The level of activated Rac1 in VLDLr-expressing MEF-2 cells, compared with vector-transfected control cells, is shown in the bar graph (mean ± SEM, $n = 3$). The asterisk indicates statistical significance (unpaired t test, $P < 0.05$). (C) uPAR-deficient A1 cells and uPAR-expressing C1 cells were cultured in the absence (−) or presence (+) of 200 nM GST-RAP for 3 d. Rac1 activation was then determined. The values shown in the bar graph are standardized against uPAR−/− cells that were not treated with RAP (mean ± SEM, $n = 3$). The asterisk indicates a statistical significance between C1 cells that were cultured in the presence and absence of RAP (unpaired t test, $P < 0.05$). (D) LM-TK$^-$ and L929 cells were cultured in the presence or absence of 200 nM GST-RAP for 3 d. Rac1 activation was then determined. The bar graph shows values that were standardized against activated Rac1 in LM-TK$^-$ cells or L929 cells that were not RAP-treated (mean ± SEM, $n = 3$). The asterisk indicates that Rac1 activation in L929 cells treated with RAP was significantly different from Rac1 activation in the same cells that were not treated with RAP (unpaired t test, $P < 0.05$). In control experiments, we demonstrated that GST does not affect Rac1 activation (not depicted).

the MEF-1 or MEF-2 cells. By contrast, N17Rac1 selectively inhibited MEF-2 cell migration, reducing the rate to that observed with MEF-1 cells. These results and the results of our experiments with uPAR+/+ and uPAR−/− MEFs demonstrate the importance of Rac1 in regulating MEF migration. Furthermore, these results demonstrate that regulation of Rac1 by LRP-1 affects an important physiologic property of the cell.

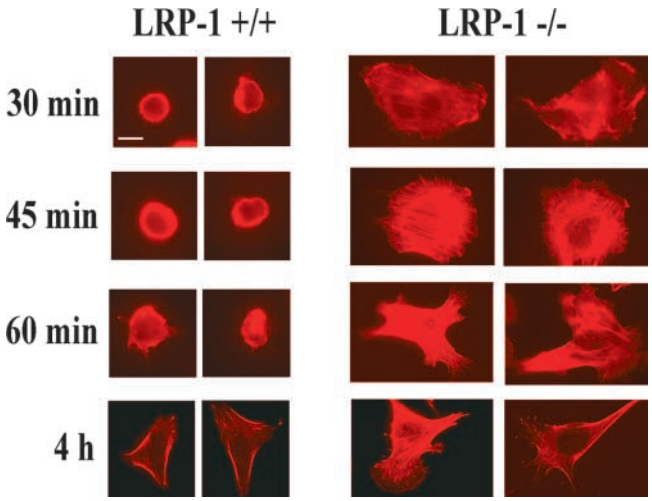

Figure 7. **The morphology of LRP-1-expressing and -deficient MEFs.** MEF-1 and MEF-2 cells were plated in serum-coated chamber slides for the indicated times and stained with rhodamine-conjugated phalloidin. Images were collected using the fluorescence microscope. Bar, 10 μm.

LRP-1 does not regulate cell migration in uPAR-deficient cells

Our uPAR−/− MEFs provided an opportunity to probe for uPAR-independent mechanisms whereby LRP-1 may regulate cell migration. When cultured in the presence of RAP for 3 d, uPAR-deficient MEFs (A1 and A2 cells) failed to demonstrate altered cell migration (Fig. 9 A). Under the same treatment conditions, uPAR+/+ and uPAR+/− cells demonstrated increased migration, as was anticipated due to the effects of RAP on Rac1 activation.

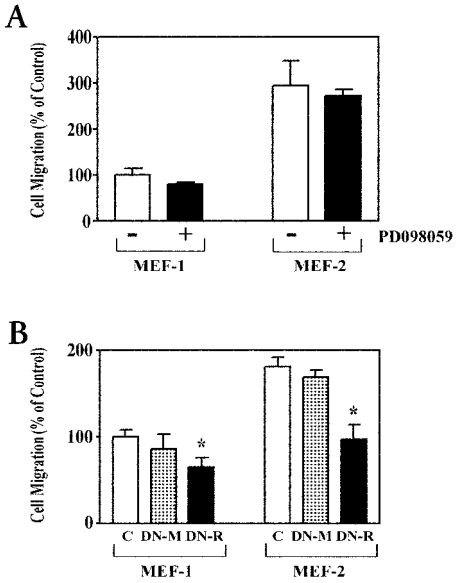

Figure 8. **ERK and Rac1 in migration of LRP-1-deficient MEFs.** (A) MEF-1 and MEF-2 cells were treated with 10 μM of the MEK inhibitor, PD098059 or with vehicle (DMSO) for 15 min at RT, and were then allowed to migrate through serum-coated Transwell membranes. The number of migrating cells was determined by crystal violet staining. (B) MEF-1 and MEF-2 cells were cotransfected to express dominant-negative MEK1 (DN-M) or dominant-negative Rac1 (DN-R) and GFP. Control cells were transfected with empty vector (pBK-CMV) and pEGFP-N1. Cell migration experiments were performed 24 h after transfection. Migration was determined by fluorescence microscopy. Results are expressed relative to the migration rate in MEF-1 cells transfected with pBK-CMV and pEGFP-N1 ($n = 4$). The asterisk indicates statistical significance at the $P < 0.05$ level.

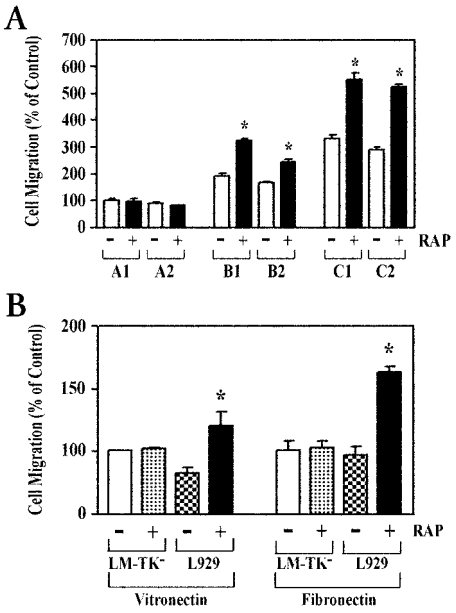

Figure 9. **Effects of LRP-1 neutralization on MEF migration in the absence of uPAR.** (A) uPAR−/− (A1 and A2), uPAR+/− (B1 and B2), and uPAR+/+ (C1 and C2) MEFs were cultured in the presence or absence of 200 nM GST-RAP for 3 d. Cells were allowed to migrate through Transwell membranes that were precoated with FBS. Migration was determined by crystal violet staining. The asterisk indicates that the bar is significantly different from the control (no RAP treatment; unpaired *t* test, $P < 0.01$, $n = 3$). (B) Migration of LM-TK⁻ and L929 cells was studied after culturing these cells in the presence or absence of GST-RAP for 3 d. Cells were allowed to migrate through Transwell membranes that were precoated with vitronectin or fibronectin. Cell migration was determined by crystal violet staining. The asterisk indicates statistical significance (unpaired *t* test, $P < 0.01$; $n = 3$).

Identical experiments were performed with LM-TK⁻ and L929 cells. Because LM-TK⁻cells lack all GPI-anchored proteins in addition to uPAR, this system is less specific than the MEF system. However, when LM-TK⁻ cells were cultured in the presence of RAP for 3 d, cell migration was unchanged (Fig. 9 B). By contrast, RAP treatment promoted L929 cell migration on vitronectin. Interestingly, L929 cell migration on fibronectin was also promoted. Thus, in two separate model systems, neutralizing the activity of LRP-1 failed to affect cell migration when uPAR is not present.

Discussion

LRP-1 gene deletion in mice is embryonic lethal (Herz et al., 1992), and the lethality has not been explained. Conditional LRP-1 gene targeting in the liver, using the Cre–loxP system, demonstrated a role for LRP-1 in the clearance of chylomicron remnants (Rohlmann et al., 1998); however, other LRP-1 functions were not addressed. Understanding the function of LRP-1 at the level of the cell may provide im-

portant clues as to the function of this receptor in normal physiology and in disease.

Cell migration is critical in embryonic development and in both physiologic and pathophysiologic processes in the adult, including inflammation, wound repair, atherogenesis, and cancer invasion (Horwitz and Parsons, 1999). Within the cell, signaling cascades that regulate cell migration may be compartmentalized so that different signals impact on processes occurring at the leading edge, in the cell body, and in the trailing uropod. Signaling proteins that function preferentially at the leading edge, including Rac1, typically regulate new actin polymerization (Kraynov et al., 2000; Ridley et el., 2001). RhoA and its downstream effector, Rho kinase, may act selectively in the uropod by loosening integrin-based adhesions (Worthylake et al., 2001). The subcellular sites where ERK and MLCK function are less clear. These proteins may have a role in uropod retraction; however, MLCK has been selectively localized to lamellipodia, indicating a potentially important role in promoting contractility at this site (Chew et al., 2002). Evidence presented here and in our previous work (Webb et al., 2000) demonstrates that LRP-1 suppresses activation of both Rac1 and the Ras-ERK pathway and may therefore inhibit cell migration by regulating two distinct signaling pathways.

The function of LRP-1 as a major regulator of the basal level of Rac1 activation is based on its ability to mediate uPAR endocytosis and substantially down-regulate cell-surface uPAR (Conese et al., 1995). LRP-1 gene neutralization in MEFs is associated with a 2.4-fold increase in cell-surface uPAR (Weaver et al., 1997). Similarly, LRP-1 antisense RNA expression in HT 1080 cells increases cell-surface uPAR by 2.4-fold (Webb et al., 2000), and neutralizing the activity of the VLDLr with RAP in MCF-7 cells increases cell-surface uPAR by threefold (Webb et al., 1999). These results suggest that the effects of LRP-1 and the VLDLr on cell-surface uPAR are similar, and the method used to neutralize these LRFs does not significantly affect the magnitude of the subsequent increase in cell-surface uPAR. LRP-1 decreases the amount of uPAR available to bind to vitronectin, which is apparently the event responsible for Rac1 activation (Kjoller and Hall, 2001).

In their original work, Kjoller and Hall (2001) overexpressed uPAR in Swiss 3T3 cells, NIH 3T3 cells, and COS-7 cells and demonstrated morphologic changes consistent with Rac1 activation. They also directly demonstrated increased GTP-bound Rac1 in uPAR-overexpressing NIH 3T3 cells. Unpublished studies from our laboratory have demonstrated that COS-7 cells express very low levels of cell-surface uPAR; however, murine fibroblasts typically express higher amounts. Thus, the activities observed by Kjoller and Hall (2001) probably represent the effects of uPAR, produced by the expression vector, superimposed on the activity of naturally occurring uPAR. Our experiments with MEFs prepared from gene knockout embryos demonstrate that naturally occurring uPAR is also an important regulator of Rac1 activation. Overexpression is not necessary to observe this activity. uPAR$-/-$ MEFs demonstrated a substantial decrease in Rac1 activation, decreased migration on vitronectin, and altered morphology, consistent with Rac1 deactivation.

Regulation of Rac1 by LRP-1 was observed in serum-containing medium. By contrast, the effects of LRP-1 on ERK activation were observed only in serum-free medium. The ability of serum to override the function of LRP-1 as a regulator of ERK stresses the importance of the cellular microenvironment in determining the activity level of signaling proteins, such as ERK, which serve as convergence points for numerous pathways initiated by integrins and growth factor receptors (Schwartz and Ginsberg, 2002). In multicellular tissues, LRP-1–expressing cells may be exposed to growth factors and regulatory molecules that differ from those present in serum or in medium that is conditioned by a single cell type. Furthermore, the concentration of uPA in the microenvironment of the cell will be influenced not only by the cell that expresses the uPA, but also by other cells that express uPAR and/or LRFs capable of uPA catabolism. These factors may all contribute in determining whether LRP-1 regulates ERK in vivo.

Although for the most part, our data support a model in which ligation of vitronectin is necessary for uPAR signaling to Rac1, some inconsistent results remain to be clarified. For example, we previously demonstrated that when cultured on fibronectin-coated surfaces, LRP-1–deficient MEF-2 cells demonstrate increased migration compared with MEF-1 cells (Weaver et al., 1997). Similarly, in this paper, we demonstrated that RAP-treated L929 cells migrate at an increased rate not only on vitronectin-coated surfaces, but also on fibronectin-coated surfaces. The role of Rac1 in mediating these LRP-1–dependent changes when vitronectin is not available to bind uPAR remains to be established.

An intimate relationship between LRP-1 (or the VLDLr) and the uPA–uPAR system in regulating cell signaling and migration has now been established in MEFs, fibroblasts, fibrosarcoma cells, and in some carcinoma cells. Although the effects of uPAR and LRP-1 on cell migration may be cell type-specific, conserved properties have emerged. LRP-1 down-regulates the uPA–uPAR system by promoting catabolism of both uPA and uPAR (Kounnas et al., 1993; Conese et al., 1995; Webb et al., 1999). With regard to this function, studies presented here and elsewhere (Webb et al., 2000) suggest that LRP-1 and the VLDLr are interchangeable. When LRP-1 is neutralized, the concentration of uPAR in the plasma membrane increases; however, a new equilibrium is established in which alternative uPAR catabolic pathways are operational (Nykjaer et al., 1998; Webb et al., 1999). The increase in cell-surface uPAR results in activation of downstream cell-signaling pathways.

Because of our focus on cell migration and because we design many of our experiments to analyze cell signaling in the absence of exogenously added growth factors or stimulatory molecules, our results regarding the effects of LRP-1 on cell physiology have consistently revealed the potency of the uPA–uPAR system. If LRP-1 regulates a receptor other than uPAR that is involved in cell migration, this activity may not have been detected in our experiments if the required ligand was not present in the serum added to the lower Transwell chamber or produced by the cells themselves. There is growing evidence for uPAR-independent pathways by which LRP-1 regulates cell physiology. For example, by binding cJun NH_2-terminal kinase in complex with JNK-interacting

proteins, LRP-1 may regulate cell growth and apoptosis (Lutz et al., 2002). Furthermore, by binding platelet-derived growth factor BB, LRP-1 may regulate the function of PDGF β receptor (Boucher et al., 2002; Loukinova et al., 2002). In smooth muscle cells, neutralizing the activity of LRP-1 with RAP inhibits cell migration (Okada et al., 1996; Wijnberg et al., 1997), which is the reverse effect compared with what we have observed in other cell types. Thus, smooth muscle cells may represent an important model system for identifying uPAR-independent mechanisms whereby LRP-1 regulates cell physiology.

Materials and methods

Antibodies and reagents

[Glu^1]plasminogen was purified from human plasma by the method of Deutsch and Mertz (1970). Vitronectin was purified by the method of Yatohogo et al. (1988), and fibronectin by the method of Ruoslahti et al. (1982). Type I collagen was purchased from Collaborative Biochemical Products. GST-RAP was expressed and purified as described previously (Webb et al., 1999). Recombinant GST was prepared for control experiments. mAb 11H4, which recognizes the 85-kD LRP-1 light chain (Kowal et al., 1989), was purified from ascites fluid after inoculation of hybridoma cells obtained from the American Type Culture Collection (ATCC). Phospho-ERK–specific antibody and the MEK inhibitor PD098058 were purchased from Calbiochem. Total ERK was detected using an antibody purchased from Zymed Laboratories. Rac1-specific mAb was purchased from BD Biosciences. Peroxidase-conjugated anti–rabbit IgG and anti–mouse IgG were purchased from Sigma-Aldrich.

Rac/Cdc42 assay reagent, which includes residues 67–150 of p21-activated kinase fused to GST and coupled to glutathione-agarose was purchased from Upstate Biotechnology. The expression vector pRSVBneoTAg, which encodes SV40 large T antigen, was provided by Dr. Jim Pipas (University of Pittsburgh, Pittsburgh, PA). pEGFP-N1, which encodes GFP, was purchased from CLONTECH Laboratories, Inc. pKH3-N17Rac1, which encodes dominant-negative Rac1 (S17 → N; N17Rac1), was provided by Dr. Ian Macara (University of Virginia, Charlottesville, VA). The VLDLr expression construct in pRc/CMV (pRc/VLDLr) and VLDLr-specific pAb were provided by Drs. Keith McCrae and Matt Gafvels (Case Western Reserve University, Cleveland, OH). pBABE-DN-MEK1, which encodes dominant-negative rabbit MEK1 (S217 → A; DN-MEK1), was provided by Dr. Andrew Catling (University of Virginia). LipofectAMINE™ was provided by Invitrogen. VLK-*p*NA was purchased from Chromogenix.

Cell lines

LRP-1–deficient MEFs (referred to interchangeably as MEF-2 or PEA-13 cells in the literature) and LRP-1–expressing MEF-1 cells were obtained from the ATCC and cultured in DME with 10% FBS and penicillin/streptomycin. Murine L929 and LM-TK$^-$ fibroblasts also were obtained from the ATCC and cultured in the same medium. LM-TK$^-$ cells are derived from L929 cells, but lack critical genes for the proper formation of GPI anchors (Singh et al., 1991).

uPAR gene knockout mice that have been described previously (Dewerchin et al., 1996) were obtained from Dr. Peter Carmeliet (KU Leuven, Belgium). These mice were crossbred with wild-type C57B16/J mice (Jackson ImmunoResearch Laboratories). The resulting uPAR(+/−) mice were then crossbred to generate uPAR(+/+), uPAR(+/−), and uPAR(−/−) embryos that were killed at post-implantation day 12.5–14.5. Primary embryonic fibroblasts were prepared essentially as described previously (Herz et al., 1992), using torsos from which the heads and livers had been removed. The cells were cultured in DME with 10% FBS. Genotypes were established for individual embryos by semi-quantitative PCR, using genomic DNA extracted from embryonic livers. The PCR primers for uPAR amplify a template in exon 3 (Bugge et al., 1996). As an internal reference, a template from exon 2 in the PAI-1 gene was amplified using the primers 5′-CCTCATCCTGGGCCTGGTTCTGGTCT-3′ and 5′-GGTTTTC-CCCGCTGTGGTCATCTGC-3′. Further confirmation of the genotypes was obtained by performing PCR for the neo insert (present only when the gene is absent) as well as by Southern blot analysis. For Southern blots, DNA was digested with BamHI, subjected to electrophoresis on 0.8% agarose gels, and probed with a fragment of the neo gene that detects a 5.5-kb band.

MEFs from uPAR+/+, uPAR+/−, and uPAR−/− embryos were immortalized by transfection to express SV-40 large T antigen. Transfected cells were selected for 3 wk in 1 mg/ml G418. A1 cells (uPAR−/−), B1 cells (uPAR+/−), and C1 cells (uPAR+/+) were derived from embryos of a single breeding. A2 cells (uPAR−/−), B2 cells (uPAR+/−), and C2 cells (uPAR+/+) were from separate litters.

Transient transfection protocols

For cell migration experiments, MEF-1, MEF-2, uPAR+/+, uPAR+/−, and uPAR−/− MEFs (3×10^5) were cotransfected with constructs encoding 1.5 μg dominant-negative MEK1 or 1.5 μg dominant-negative Rac1 and 0.5 μg of pEGFP-N1 by incubation for 4.5 h with 12 μl LipofectAMINE™. Control cells were cotransfected with empty vector (pBK-CMV) and pEGFP-N1. Transfected cells were cultured for 24 h before analysis. For Rac1 activation experiments, MEF-2 cells (6×10^5) were transfected with pRc/VLDLr, pRc/CMV, or pEGFP-N1 (6 μg) using 36 μl LipofectAMINE™. Transfection efficiencies were >80%, as determined by counting green fluorescent cells in preparations transfected with pEGFP-N1. Cotransfection efficiencies were determined as described previously (Nguyen et al., 1999), and were always essentially 100%.

Activity assay for the determination of cell-surface uPAR

MEF-2 cells, which provide a rich source of murine uPA (Weaver et al., 1997), were cultured in serum-free DME for 24 h. Conditioned medium was collected and subjected to centrifugation at 2,000 *g* to remove cellular debris and then concentrated 20-fold using Centricon concentrators with 10-kD exclusion filters (Amicon; Millipore).

L929 cells, LM-TK$^-$ cells, uPAR+/+ MEFs, uPAR+/− MEFs, and uPAR−/− MEFs were plated at 2.8×10^5 cells/well in 24-well plates and cultured overnight. The cells were subjected to a mild acid wash as described previously (Ma et al., 2001), and were then incubated with concentrated conditioned medium from MEF-2 cells for 1 h at 4°C. After washing the cultures three times with Earle's balanced salt solution, 25 mM Hepes, and 5 mg/ml BSA, pH 7.4, the cells were reconstituted in 1 ml of the same buffer supplemented with 1 μM [Glu^1]plasminogen and 0.5 mM VLK-*p*NA. 0.5 mM amiloride was added to some cultures to specifically inhibit uPA and not tissue-type plasminogen activator (Weaver et al., 1997). Plasminogen activation was allowed to proceed for 3 h at 37°C. Hydrolysis of VLK-*p*NA was detected by measuring the absorbance at 405 nm. To standardize the activity assay, cellular protein was determined by fluoraldehyde assay.

Cell migration assays

6.5-mm Transwell membranes (8.0-μm pores; Costar) were coated on the underside only with 20% FBS, 5 μg/ml purified vitronectin, 10 μg/ml fibronectin, or 25 μg/ml type I collagen for 2 h at 37°C. Vitronectin is the principal protein that coats membranes that are treated with FBS (Hayman et al., 1985). Both membrane surfaces were blocked with 5 mg/ml BSA. Cells were dissociated from monolayer culture, washed in serum-free medium, and transferred to the top chamber of each Transwell unit at a density of 10^6 cells/ml in 100 μl DME. The bottom chamber contained DME and 10% FBS. Some cells were pretreated for 15 min with 10 μM of the MEK inhibitor PD098059. Other cells were cultured for 3 d in medium supplemented with 200 nM GST-RAP or GST. When these protocols were executed, the same agent (GST-RAP or PD098059) was added to both Transwell chambers. Migration was allowed to proceed for 6 h at 37°C. Nonmigrating cells were removed from the top surfaces of the Transwell membranes using cotton swabs. The membranes were then fixed in methanol and stained with 0.1% crystal violet. The dye was eluted with 10% acetic acid, and the absorbance of the eluate was determined at 570 nm. In control experiments, we confirmed that crystal violet absorbance is a linear function of cell number.

To study migration of GFP-expressing cells, translucent BioCoat™ Cell Culture Inserts (BD Biosciences) were used instead of Transwell chambers. The insert membranes had 8-μm pores and were coated on the underside surfaces with 20% FBS. Cells that were cotransfected with signaling effector mutants and pEGFP-N1 or with empty vector and pEGFP-N1 were added to the top chamber and allowed to migrate for 4 h at 37°C. Nonmigrating cells were removed and the membranes were fixed in 4% PFA. Migrating cells were then counted by fluorescence microscopy.

ERK activation

Phosphorylated and total ERK were detected by immunoblot analysis. Subconfluent cultures were incubated in serum-containing or serum-free medium for the indicated times. The medium was then replaced with 20 mM

ice-cold sodium phosphate, 150 mM NaCl, pH 7.4, containing 1 mg/ml sodium orthovanadate. Cells were extracted in 1.0% NP-40, 50 mM Hepes, 100 mM NaCl, 2 mM EDTA, 1 μg/ml leupeptin, 100 KIU/ml aprotinin, 0.4 mg/ml sodium orthovanadate, 0.4 mg/ml sodium fluoride, and 5 mg/ml dithiothreitol, pH 7.4. Equal amounts of cell extract were subjected to SDS-PAGE on 10% slabs. Proteins were transferred to nitrocellulose membranes and probed with antibodies that detect phosphorylated and total ERK. Primary antibodies were detected using peroxidase-conjugated anti–rabbit IgG and ECL.

Rac1 activation

Under our standard conditions, cells were maintained for 18 h after plating in 10% FBS-supplemented medium before performing assays to detect activated Rac1. In some experiments, cells were cultured in the presence or absence of 200 nM GST-RAP for 3 d. The medium was changed every day and fresh GST-RAP was added.

Cell extracts were prepared at 4°C from equal amounts of cell protein, using prechilled GST-PAK-CRIB assay buffer (50 mM Tris-HCl, pH 7.4, 2 mM $MgCl_2$, 1% vol/vol NP-40, 10% glycerol, 100 mM NaCl, 1 μg/ml leupeptin, 100 KIU/ml aprotinin, 0.4 mg/ml sodium orthovanadate, and 0.4 mg/ml sodium fluoride). Extracts were cleared by centrifugation at 11,000 *g* for 2 min at 4°C in the presence of Sepharose CL-4B. 30-μl samples were withdrawn for analysis of total Rac1. The remainder of each extract was incubated for 45 min at 4°C with 7.5 μl of p21-activated kinase-PBD agarose (50% slurry), which selectively binds the active or GTP-loaded forms of Rac and Cdc42. The beads were washed three times with assay buffer and eluted with SDS-PAGE sample buffer. The eluates were then subjected to immunoblot analysis using Rac1-specific antibody.

Fluorescence microscopy

MEF-1, MEF-2, uPAR+/+ C1 cells, and uPAR−/− A1 cells were plated in serum-coated chamber slides (10^4 cell per well) for the indicated times (0.5–4 h) and fixed in 4% PFA for 20 min at 25°C. After fixation, cells were permeabilized with 0.2% Triton X-100 and then blocked with 20% goat serum in 20 mM sodium phosphate, 150 mM NaCl, pH 7.4 (PBS), for 1 h at 25°C. The cells were then incubated for 1 h at 25°C with rhodamine-conjugated phalloidin (1:500 dilution; Molecular Probes, Inc.) in PBS with 5% goat serum. Fluorescence microscopy was performed using a rhodamine/TRITC cube (excitation BP520–550, barrier filter BA580IF, dichroic mirror DM565). Images were collected using a cooled CCD camera (Orca II; Hamamatsu Corporation) attached to a Nikon TE-300 inverted microscope with a 60× objective (NA 1.4).

The authors would like to thank Kari Nejak for outstanding technical assistance and Dr. Jeffrey Lysiak and Jennifer Kirby for helpful input into the initiation of this project.

This work was supported by National Institutes of Health grants HL-60551 and CA-94900.

Submitted: 12 July 2002
Revised: 14 November 2002
Accepted: 14 November 2002

References

Aguirre-Ghiso, J.A., K. Kovalski, and L. Ossowski. 1999. Tumor dormancy induced by downregulation of urokinase receptor in human carcinoma involves integrin and MAPK signaling. *J. Cell Biol.* 147:89–103.

Barnes, H., B. Larsen, M. Tyser, and P. van der Geer. 2001. Tyrosine-phosphorylated low density lipoprotein receptor-related protein 1 (LRP-1) associates with the adaptor protein SHC in Src-transformed cells. *J. Biol. Chem.* 276: 19119–19125.

Boucher, P., P. Liu, M. Gotthardt, T. Hiesberger, R.G.W. Anderson, and J. Herz. 2002. Platelet-derived growth factor mediates tyrosine phosphorylation of the cytoplasmic domain of low density lipoprotein receptor-related protein in caveolae. *J. Biol. Chem.* 277:15507–15513.

Bugge, T.H., T.T. Suh, M.J. Flick, C.C. Daugherty, J. Romer, H. Solberg, V. Ellis, K. Dano, and J.L. Degen. 1996. The receptor for urokinase-type plasminogen activator is not essential for mouse development or fertility. *J. Biol. Chem.* 270:16886–16894.

Chew, T.-L., W.A. Wolf, P.J. Gallagher, F. Matsumura, and R.L. Chisolm. 2002. A fluorescent resonant energy transfer-based biosensor reveals transient and regional myosin light chain kinase activation in lamella and cleavage furrows. *J. Cell Biol.* 156:543–553.

Conese, M., A. Nykjaer, C.M. Petersen, O. Cremona, R. Pardi, P.A. Andreasen, J. Gliemann, E.I. Christensen, and F. Blasi. 1995. α_2-Macroglobulin receptor/LDL receptor-related protein (LRP)-dependent internalization of the urokinase receptor. *J. Cell Biol.* 13:1609–1622.

D'Arcangelo, G., R. Homayouni, L. Keshvara, D.S. Rice, M. Sheldon, and T. Curran. 1999. Reelin is a ligand for lipoprotein receptors. *Neuron.* 24:471–479.

Dewerchin, M., A.N. Nuffelen, G. Wallays, A. Bouche, L. Moons, and P. Carmeliet. 1996. Generation and characterization of urokinase receptor-deficient mice. *J. Clin. Invest.* 97:870–878.

Deutsch, D.G., and E.T. Mertz. 1970. Plasminogen: purification from human plasma by affinity chromatography. *Science.* 170:1095–1096.

Goldstein, J.L., R.G.W. Anderson, and M.S. Brown. 1979. Coated pits, coated vesicles, and receptor-mediated endocytosis. *Nature.* 279:679–684.

Gotthardt, M., M. Trommsdorff, M.F. Nevitt, J. Shelton, J.A. Richardson, W. Stockinger, J. Nimpf, and J. Herz. 2000. Interactions of the low density lipoprotein receptor gene family with cytosolic adaptor and scaffold proteins suggest diverse biological functions in cellular communication and signal transduction. *J. Biol. Chem.* 275:25616–25624.

Hamik, A., H. Setiadi, G.J. Bu, R.P. McEver, and J.H. Morrissey. 1999. Down-regulation of monocyte tissue factor mediated by tissue factor pathway inhibitor and the low density lipoprotein receptor-related protein. *J. Biol. Chem.* 274:4962–4969.

Hayman, E.G., M.D. Pierschbacker, S. Suzuki, and E. Ruoslahti. 1985. Vitronectin – a major cell attachment-promoting protein in fetal bovine serum. *Exp. Cell Res.* 160:245–258.

Herz, J., D.E. Clouthier, and R.E. Hammer. 1992. LDL receptor-related protein internalizes and degrades uPA-PAI-1 complexes and is essential for embryo development. *Cell.* 71:411–421.

Horwitz, A.R., and J.T. Parsons. 1999. Cell migration – movin' on. *Science.* 286: 1102–1103.

Kinoshita, A., C.M. Whelan, C.J. Smith, I. Mikhailenko, G.W. Rebeck, D.K. Strickland, and B.T. Hyman. 2001. Demonstration by fluorescence resonance energy transfer of two sites of interaction between the low-density lipoprotein receptor-related protein and the amyloid precursor protein: role of the intracellular adapter protein Fe65. *J. Neurosci.* 21:8354–8361.

Kjoller, L., and A. Hall. 2001. Rac mediates cytoskeletal rearrangements and increased cell motility induced by urokinase-type plasminogen activator receptor binding to vitronectin. *J. Cell Biol.* 152:1145–1157.

Klemke, R.L., S. Cai, A.L. Giannini, P.J. Gallagher, P. de Lanerolle, and D.A. Cheresh. 1997. Regulation of cell motility by mitogen activated protein kinase. *J. Cell Biol.* 137:481–492.

Knauer, M.F., S.J. Kridel, S.B. Hawley, and D.J. Knauer. 1997. The efficient catabolism of thrombin-protease nexin 1 complex is a synergistic mechanism that requires both the LDL receptor-related protein and cell surface heparins. *J. Biol. Chem.* 272:29039–29045.

Kounnas, M.Z., J. Henkin, W.S. Argraves, and D.K. Strickland. 1993. Low density lipoprotein receptor-related protein/α_2-macroglobulin receptor mediates cellular uptake of pro-urokinase. *J. Biol. Chem.* 268:21862–21867.

Kowal, R.C., J. Hertz, J.L. Goldstein, V. Esser, and M.S. Brown. 1989. Low density lipoprotein receptor-related protein mediates uptake of cholesteryl esters derived from apoprotein E-enriched lipoproteins. *Proc. Natl. Acad. Sci. USA.* 86:5810–5814.

Kraynov, V.S., C. Chamberlain, G.M. Bokoch, M.A. Schwartz, S. Slabaugh, and K.M. Hahn. 2000. Localized Rac activation dynamics visualized in living cells. *Science.* 290:333–337.

Li, Y., W. Lu, P. Marzolo, and G. Bu. 2001. Differential functions of members of the low density lipoprotein receptor family suggested by their distinct endocytosis rates. *J. Biol. Chem.* 276:18000–18006.

Loukinova, E., S. Ranganathan, S. Kuznetsov, N. Gorlatova, M.M. Migliorini, D. Loukinov, P.G. Ulery, I. Mikhailenko, D.A. Lawrence, and D.K. Strickland. 2002. Platelet-derived growth factor-induced tyrosine phosphorylation of the low density lipoprotein receptor-related protein. *J. Biol. Chem.* 277: 15499–15506.

Lutz, C., J. Nimpf, M. Jenny, K. Boecklinger, C. Enzinger, G. Utermann, G. Baier-Bitterlich, and G. Baier. 2002. Evidence of functional modulation of the MEKK/JNK/cJun signaling cascade by the low density lipoprotein receptor-related protein (LRP). *J. Biol. Chem.* 277:43143–43151.

Ma, Z., D.J. Webb, M. Jo, and S.L. Gonias. 2001. Endogenously produced urokinase-type plasminogen activator is a major determinant of the basal level of activated ERK/MAP kinase and prevents apoptosis in MDA-MB-231 breast cancer cells. *J. Cell Sci.* 114:3387–3396.

Nguyen, D.H.D., A.D. Catling, D.J. Webb, M. Sankovic, L.A. Walker, A.V. Somlyo, M.J. Weber, and S.L. Gonias. 1999. Myosin light chain kinase functions downstream of Ras/ERK to promote migration of urokinase-type plasminogen activator-stimulated cells in an integrin-selective manner. *J. Cell Biol.* 146:149–164.

Nykjaer, A., E.I. Christensen, H. Vorum, H. Hager, C.M. Petersen, H. Roigaard, H.Y. Min, F. Vilhardt, L.B. Moller, S. Kornfeld, and J. Gliemann. 1998. Mannose 6-phosphate/insulin-like growth factor-II receptor targets the urokinase receptor to lysosomes via a novel binding interaction. *J. Cell Biol.* 141:815–828.

Okada, S.S., S.R. Grobmyer, and E.S. Barnathan. 1996. Contrasting effects of plasminogen activators, urokinase receptor, and LDL receptor-related protein on smooth muscle cell migration and invasion. *Arterioscler. Thromb. Vasc. Biol.* 16:1269–1276.

Ossowski, L., and J. Aguirre-Ghiso. 2000. Urokinase receptor and integrin partnership: coordination of signaling and cell adhesion, migration and growth. *Curr. Opin. Cell Biol.* 12:613–620.

Ridley, A.J. 2001. Rho GTPases and cell migration. *J. Cell Sci.* 114:2713–2722.

Rohlmann, A., M. Gotthardt, R.E. Hammer, and J. Herz. 1998. Inducible inactivation of hepatic LRP gene by Cre-mediated recombination confirms role of LRP in clearance of chylomicron remnants. *J. Clin. Invest.* 101:689–695.

Ruoslahti, E., E.G. Hayman, M. Pierschbacher, and E. Engvall. 1982. Fibronectin: purification, immunochemical properties, and biological activities. *Methods Enzymol.* 82:803–831.

Salicioni, A.M., K.S. Mizelle, E. Loukinova, I. Mikhailenko, D.K. Strickland, and S.L. Gonias. 2002. The low density lipoprotein receptor-related protein mediates fibronectin catabolism and inhibits fibronectin accumulation on cell surfaces. *J. Biol. Chem.* 277:16160–16166.

Schwartz, M.A., and M.H. Ginsberg. 2002. Networks and crosstalk: integrin signaling spreads. *Nat. Cell Biol.* 4:E65–E68.

Singh, N., D. Singleton, and A.M. Tartakoff. 1991. Anchoring and degradation of glycolipid-anchored membrane proteins by L929 versus by LM-TK$^-$ mouse fibroblasts: implications for anchor biosynthesis. *Mol. Cell. Biol.* 11:2362–2374.

Strickland, D.K., S.L. Gonias, and W.S. Argraves. 2002. Diverse roles for the LDL receptor family. *Trends Endocrinol. Metab.* 13:66–74.

Su, H.P., K. Nakada-Tsukui, A.-C. Tosello-Trampon, Y.H. Li, G.J. Bu, P.M. Henson, and K.S. Ravichandran. 2002. Interaction of CED-6/GULP, an adapter protein involved in engulfment of apoptotic cells with CED-1 and CD91/low density lipoprotein receptor-related protein (LRP). *J. Biol. Chem.* 277:11772–11779.

Tamai, K., M. Semenov, Y. Kato, R. Spokony, C. Liu, Y. Katsuyama, F. Hess, J.-P. Saint-Jeannet, and X. He. 2000. LDL-receptor-related proteins in Wnt signal transduction. *Nature*. 407:530–535.

Trommsdorff, M., M. Gotthardt, T. Hiesberger, J. Shelton, W. Stockinger, J. Nimpf, R.E. Hammer, J.A. Richardson, and J. Herz. 1999. Reeler/disabled-like disruption of neuronal migration in knockout mice lacking the VLDL receptor and apoE receptor 2. *Cell.* 97:689–701.

Ulery, P.G., J. Beers, I. Mikhailenko, R.E. Tanzi, G.W. Rebeck, B.T. Hyman, and D.K. Strickland. 2000. Modulation of β-amyloid precursor protein processing by the low density lipoprotein receptor-related protein (LRP). *J. Biol. Chem.* 275:7410–7415.

Weaver, A.M., M. McCabe, I. Kim, M.M. Allietta, and S.L. Gonias. 1996. Epidermal growth factor and platelet-derived growth factor-BB induce a stable increase in the activity of low density lipoprotein receptor-related protein in vascular smooth muscle cells by altering receptor distribution and recycling. *J. Biol. Chem.* 271:24894–24900.

Weaver, A.M., I.M. Hussaini, A. Mazar, J. Henkin, and S.L. Gonias. 1997. Embryonic fibroblasts that are genetically deficient in low density lipoprotein receptor-related protein demonstrate increased activity of the urokinase receptor system and accelerated migration on vitronectin. *J. Biol. Chem.* 272: 14372–14379.

Webb, D.J., D.H.D. Nguyen, M. Sankovic, and S.L. Gonias. 1999. The very low density lipoprotein receptor regulates urokinase receptor catabolism and breast cancer cell motility *in vitro*. *J. Biol. Chem.* 274:7412–7420.

Webb, D.J., D.H.D. Nguyen, and S.L. Gonias. 2000. Extracellular signal-regulated kinase functions in the urokinase receptor-dependent pathway by which neutralization of low density lipoprotein receptor-related protein promotes fibrosarcoma cell migration and Matrigel invasion. *J. Cell Sci.* 113:123–134.

Wei, Y., D.A. Waltz, N. Rao, R.J. Drummond, S. Rosenberg, and H.A. Chapman. 1994. Identification of the urokinase receptor as an adhesion receptor for vitronectin. *J. Biol. Chem.* 269:32380–32388.

Wijnberg, M.J., P.H.A. Quax, N.M.E. Nieuwenbroek, and J.H. Verheijen. 1997. The migration of smooth muscle cells in vitro is mediated by plasminogen activation and can be inhibited by α_2-macroglobulin receptor associated protein. *Thromb. Haemost.* 78:880–886.

Worthylake, R.A., S. Lemoine, J.M. Watson, and K. Burridge. 2001. RhoA is required for monocyte tail retraction during transendothelial migration. *J. Cell Biol.* 154:147–160.

Yatohogo, T., M. Izumi, H. Kashiwagi, and M. Hayashi. 1988. Novel purification of vitronectin from human plasma by heparin affinity chromatography. *Cell Struct. Funct.* 13:281–292.

Yebra, M., G.C.N. Parry, S. Stromblad, N. Mackman, S. Rosenberg, B.M. Mueller, and D.A. Cheresh. 1996. Requirement of receptor-bound urokinase-type plasminogen activator for integrin $\alpha_v\beta_5$-directed cell migration. *J. Biol. Chem.* 271:29393–29399.